

Enantioseparation of mandelic acid and substituted derivatives by high-performance liquid chromatography with hydroxypropyl- β -cyclodextrin as chiral mobile additive and evaluation of inclusion complexes by molecular dynamics

Jie-Hua Shi  | Zhen-Yi Lin | Song-Bo Kou | Bao-Li Wang | Shao-Liang Jiang

College of Pharmaceutical Science,
Zhejiang University of Technology,
Hangzhou, P.R. China

Correspondence

Jie-Hua Shi and Shao-Liang Jiang, College
of Pharmaceutical Science, Zhejiang
University of Technology, 18, Chaowang
Road, Hangzhou, P.R. China.
Email: shijh@zjut.edu.cn;
shljiang@zjut.edu.cn

Funding information

Huahai Pharmaceutical Co., Ltd., Grant/
Award Number: YX-KF-[2005]018

Abstract

The enantioseparation and resolution mechanism of mandelic acid (MA), 4-methoxymandelic acid (MMA), and 4-propoxymandelic acid (PMA) were investigated by reversed-phase high-performance liquid chromatography (HPLC) with 2-hydroxypropyl- β -cyclodextrin (HP- β -CD) as a chiral mobile-phase additive and molecular dynamics simulation. The suitable chromatographic conditions for the enantioseparation of MA, MMA, and PMA were obtained. Under the selected chromatographic conditions, these enantiomers could achieve baseline separation. The results of thermodynamic parameter analysis revealed that the main driven forces for the enantioseparation of MA, MMA, and PMA could be van der Waals forces and hydrogen-bonding interactions and the chromatographic retention of these chiral compounds was an enthalpy-driven process. The results of the molecular simulation revealed that their chiral resolution mechanism on HP- β -CD was responsible for the formation of inclusion complexes of enantiomers with HP- β -CD with different conformations and binding energies. And the binding energy of HP- β -CD with (*S*)-isomer was larger than that with (*R*)-isomer, which is consistent with the experimental results of the first elution of (*S*)-isomer. Additionally, it is also confirmed that the interaction energies included the van der Waals energy (ΔE_{vdw}), electrostatic energy (ΔE_{elec}), polar solvation energy, and SASA energy (ΔE_{sasa}), and the separation factor (α) was closely connected with the disparity in the binding energies of optical isomers and HP- β -CD complexes. Meanwhile, from molecular dynamics simulation, it can be found that the $\Delta(\Delta E_{binding})$, ($\Delta(\Delta E_{binding}) = \Delta E_{binding,R} - \Delta E_{binding,S}$) value was in order of MA-HP- β -CD complex > MMA-HP- β -CD complex > PMA-HP- β -CD complex, which was consistent with the order of $\Delta(\Delta G)$ values obtained from van't Hoff plot. This indicated that the molecular dynamics simulation has predictive function for chiral resolution.

KEYWORDS

4-methoxymandelic acid, 4-propoxymandelic acid, chiral recognition, cyclodextrin, HPLC, mandelic acid, molecular dynamics simulation

1 | INTRODUCTION

Since the US Food and Drug Administration (FDA) announced the guidelines for chiral drug in 1992, enantiomeric separation of chiral compounds has received much attention. Up to now, high-performance liquid chromatography (HPLC) has become an essential tool for enantiomer separation of chiral compounds in the pharmaceutical, agrochemical, perfume, textile, or food industries.¹ As is known to all, cyclodextrins, a kind of natural cyclic oligosaccharides, possess much better chiral recognition ability for many chiral compounds.^{2,3} This chiral recognition ability is responsible for which they can be easy-to-generate complexes with diverse guest molecules and thus change the nature of guest molecules.⁴ 2-Hydroxypropyl- β -cyclodextrin (HP- β -CD), one of the β -CD derivatives, possesses better chiral recognition ability and solubility in aqueous solution than native β -cyclodextrin (β -CD).⁵ Recently, HP- β -CD has been widely used as chiral selector to separate the enantiomers of chiral compounds, such as using HPLC,^{6,7} capillary electrophoresis (CE),^{8,9} enantioselective liquid-liquid extraction,¹⁰ and membrane separation.¹¹

As the important chiral building blocks and organic synthesis intermediates, mandelic acid (MA) and its derivatives are extensively utilized for pharmaceutical and fine chemical industries. For example, racemic MA was used for the biosynthesis of L-phenylglycine.¹² 2-Substituted-1,4-diketones were prepared from (*S*)-MA enolate through enantioselective synthesis.¹³ (*R*)-MA was used as an antibiotic side-chain modifier for cefidiomycetes, and (*S*)-MA is a precursor for the synthesis of the drug (*S*)-oxibutin for the treatment of urinal urgency, frequent urination, and urinary incontinence.¹⁴ Naphthodifuranone dyes were prepared from 4-alkoxymandelic acid such as 4-propoxymandelic acid (PMA) and 4-methoxymandelic acid (MMA).¹⁵ At the same time, many studies on the chiral separation of MA and its derivatives were performed. Tong et al. reported that the optical isomers of MA derivatives were separated using chiral mobile-phase additive method.¹⁶ Tong et al. also studied the enantioseparation of MA using counter-current chromatography.¹⁷ Shi et al. investigated the separation of optical isomers of α -cyclohexylmandelic acid and methyl α -cyclohexylmandelates with HP- β -CD as chiral selector and discussed their chiral recognition

mechanism based on molecular docking.¹⁸ Shi et al. studied the chiral separation of optical isomers of methyl mandelate and methyl cyclohexylmandelate using chiral stationary phase method and explored the chiral recognition mechanism using quantum chemical calculation.¹⁹ Zhang et al. studied the chiral separation of α -cyclopentyl-mandelic acid enantiomers by continuous liquid-liquid extraction.²⁰ In short, the use of a chiral mobile-phase additive to perform the enantioseparations of MA and its derivatives is feasible. Recently, theoretical methods such as semiempirical methods, molecular mechanics (MM), and molecular dynamics (MD) are widely used to study the inclusion complexes of the CDs or their derivatives with guests and to comprehend the chiral resolution mechanism.^{18,19,21-23}

The aim of this research was to explore the chiral separation of MA, MMA, and PMA enantiomers (Figure 1) by HPLC with HP- β -CD as a chiral mobile-phase additive and to comprehend the chiral resolution mechanism at the molecular level through molecular simulations including molecular docking and MD.

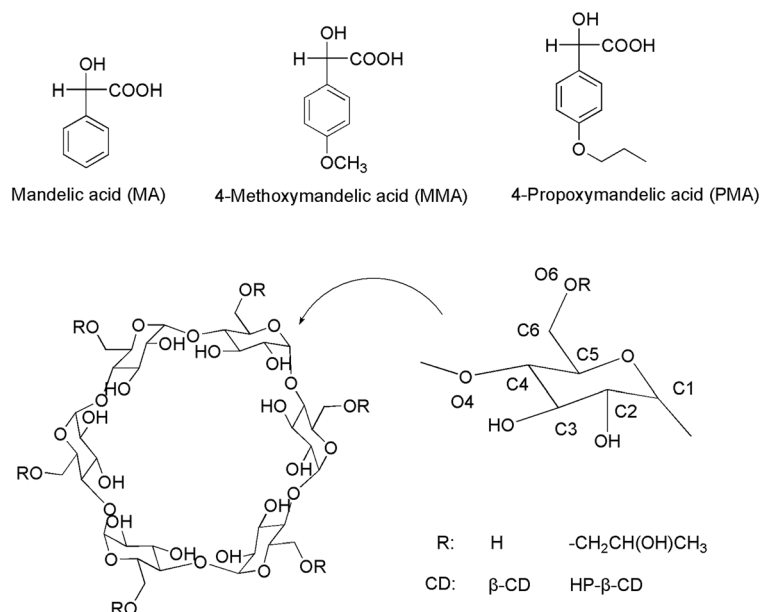
2 | MATERIALS AND METHODS

2.1 | Chemicals and solutions

MA ($\geq 99\%$) was purchased from Aladdin Chemistry Co., Ltd. (Shanghai, China). PMA ($\geq 98\%$) was purchased from Adamas-Beta Reagent, Ltd. (Shanghai, China). MMA ($\geq 97\%$) was purchased from Macklin Chemistry Co., Ltd. (Shanghai, China). HP- β -CD ($M_n = 6.4$) was provided by DELI Biochemical Industry Co., Ltd. (Xi'an, China). Phosphoric acid was obtained from Lingfeng Chemical Reagent Co., Ltd. (Shanghai, China). Sodium dihydrogen phosphate was purchased from Guanghua Sci-Tech Co., Ltd. (Guangdong, China). Acetonitrile and methanol used for HPLC analysis were of chromatographic grade. Other reagents were of analytical grade and directly used without further purification.

The HP- β -CD was dissolved in phosphate-buffered solution (PBS) (0.1 mol l^{-1}) containing HP- β -CD (15 mmol l^{-1}) and adjusted to the required pH value using phosphoric acid, which solution was used as one of the components of mobile phase and filtered using microfiltration membrane ($0.45 \mu\text{m}$) before use. All testing solutions of MA, MMA, and PMA were prepared in

FIGURE 1 Structures of MA, MMA, PMA, and HP- β -CD



anhydrous methanol with the concentration of about 2 mmol l⁻¹.

2.2 | HPLC analysis

All chromatographic separations were carried out on Waters 2695 Separations Module HPLC equipped with Waters 2996 Photodiode Array Detector and Empower 2 Chemstation workstation (Waters Corporation, Shanghai, China). XBridge™ C18 (250 × 4.6-mm i.d., 5 μ m) column was used in whole research. The mixture solution of acetonitrile and 0.1-mol l⁻¹ PBS containing 15-mmol l⁻¹ HP- β -CD was used as mobile phase. The detected wavelength and column temperature were fixed at 230 nm and 30°C, respectively. All the testing solutions of 10 μ l were injected into the HPLC for analysis.

2.3 | MD simulation

In this work, the used HP- β -CD was derived from the selective condensation reaction in position 6 of β -CD, and the mean substitution was 6.4. Therefore, we supposed the structure of HP- β -CD was mainly hepta-(6-O-(2-hydroxypropyl))- β -CD by the reference of the reported literature,^{21,22} which was used in theoretical calculation. The supposed structure of HP- β -CD was built from the coordinate of β -CD, which was extracted from the crystal structure (PDB: 1DMB) through the replacement of the H-atoms in all 6-OH with 2-hydroxypropyl group. After energetic and structural filtering to remove high-energy and redundant conformers, the resulting structure was optimized by B3LYP/6-31G(d,p) method implemented in

Gaussian 03 until no imaginary frequency and the optimized structure of HP- β -CD was represented in Figure 1.

(*R/S*)-MA and (*R/S*)-MMA were downloaded from the PubChem. (*R/S*)-PMA was constructed with the help of Gaussian view by substituting para of benzene ring of (*R/S*)-MA with propoxy group. These enantiomeric structures were optimized using DFT/B3lyp/6-31+g(d,p) approach until all eigenvalues of the Hessian matrix were positive.

The inclusion complex of HP- β -CD with various enantiomers was first simulated by semiflexible docking technique with the help of AutoDock program (Version 4.2). During molecular docking, the HP- β -CD was set as a rigid molecule, whereas guest molecules were allowed to move in free motion. A grid map with the grid points of 50 × 50 × 40 with grid spacing 0.375 Å was set to ensure that HP- β -CD is completely surrounded. Lamarckian genetic algorithm approach was used for searching the structure of inclusion complex. The running times and the number of evaluations were fixed at 500 and 2,500,000.²³ Other docking parameters were set as default. In this work, all parameters were the same for each docking. The structures of all inclusion complexes with lowest acting energy were used for the starting structure of MD simulation.

All MD simulations were performed on GROMACS program (Version 2019.3). First, the restrained electrostatic potential (RESP) of each guest molecule was calculated at DFT/B3lyp/6-311G** level. Then, each isomer with the RESP charges was parameterized by GAFF force field.²⁴ Other force field parameters came from the proposed parameters of ANTECHAMBER.^{25,26} Each inclusion complex with stoichiometric ratio of 1:1 was solvated in a regular 1.6-nm dodecahedron box with

TIP3P water containing 5% acetonitrile (v/v) model, to ensure that the whole system was dissolved in acetonitrile–water system. Next, the system was treated by energy minimization using a steepest descent integrator (50,000 steps) until the maximum force of $<10.0 \text{ kJ mol}^{-1} \text{ nm}^{-1}$ to remove the largest strains. After that, the whole system was gradually warmed to 300 K under the NVT ensemble, followed by the NPT ensemble at 1 bar. Finally, MD simulation was performed for 120 nsec in 60,000,000-step production. The representative geometry of each inclusion complex was obtained by the cluster analysis using the “gmx cluster” program. The number of collected frames was 12,000, and the balanced trajectories from 20 to 100 nsec were extracted for further analysis of interaction forces.

3 | RESULTS AND DISCUSSION

3.1 | Assessment on chromatographic conditions

3.1.1 | Influence of the type and concentration of chiral mobile-phase additive

In our exploratory experiments, β -CD, HP- β -CD, and sulfobutylether- β -CD (SBE- β -CD) were used as chiral mobile-phase additives, respectively, for the enantiomeric separation of MA, MMA, and PMA. The results revealed that their optical isomers can be efficiently resolved when HP- β -CD is used as chiral mobile-phase additives and the (*S*)-isomer was eluted before (*R*)-isomer (Figure 2). These optical isomers cannot be efficiently separated using SBE- β -CD and β -CD as chiral mobile-phase additives, although β -CD has certain chiral recognition ability to PMA. This indicates that HP- β -CD has a good chiral recognition ability for the separation of the optical isomers of MA, MMA, and PMA. In the HP- β -CD mobile-phase

additive system, (*S*)-isomer was first eluted, suggesting that the interaction of HP- β -CD with (*S*)-isomer was stronger than that with (*R*)-isomer.

Subsequently, the effect of the concentration of HP- β -CD additive on the chiral separation was investigated, and the results were summarized in Table S1. The results revealed that the capacity factors (k) decreased with the increase of the concentration of HP- β -CD whereas the separation factor (α) increased, indicating that the elution capacity is enhanced due to the solubilization effect of HP- β -CD and the separation selectivity increased. However, the resolution factor (R_s) of these enantiomers gradually declined with the increase of HP- β -CD concentration. So, considering the retention and resolution capabilities of these chiral compounds, the concentration of HP- β -CD additive (15 mmol l^{-1}) was used for the enantioseparation of these chiral compounds.

3.1.2 | Influence of pH value

As is known to all, MA, MMA, and PMA belong to strong organic acid.¹⁶ Therefore, an increase in the pH of the aqueous solution will result in a decrease in the content of free MA derivative enantiomers (electrically neutral). In addition, the chiral recognition ability of HP- β -CD is mainly related to the affinity of the neutral isomer rather than ionic isomer.²⁷ This means that the pH value of the mobile-phase affects obviously on the enantiomeric separation of acidic chiral compounds. In this work, the effect of pH values in the mobile phase containing HP- β -CD on the retention behaviors and enantioselectivity of MA, MMA, and PMA was determined, and the findings were summarized in Table S2. The finding revealed that, with the increases of pH value, the capacity factors (k_1 and k_2), separation factor (α), and resolution factor (R_s) of these enantiomers gradually decreased, which was inconsistent

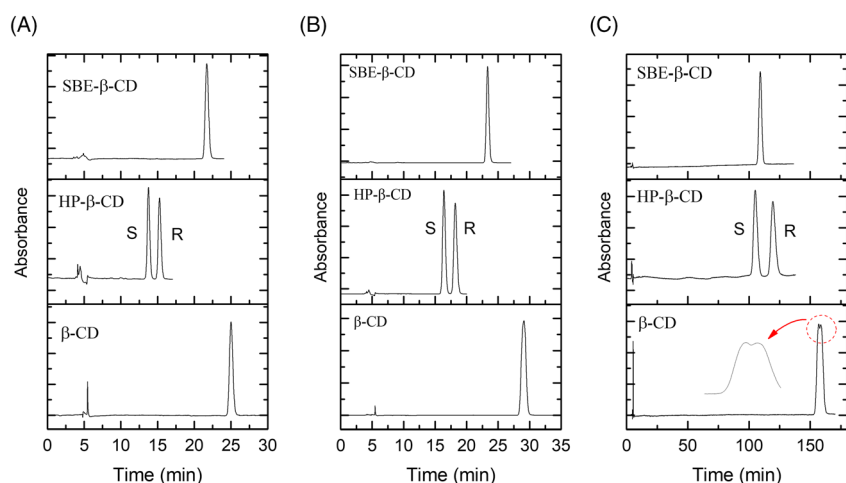


FIGURE 2 Chromatograms of the separations of (A) MA, (B) MMA, and (C) PMA enantiomers when β -CD, HP- β -CD, and SBE- β -CD as chiral mobile-phase additives. Chromatographic conditions: mobile phase: acetonitrile:PBS (0.1 mol l^{-1} , pH 2.50) containing HP- β -CD (10 mmol l^{-1}) = 5:95 (v/v). Flow rate: 0.6 ml min^{-1} ; detection wavelength: 230 nm; column temperature: 30°C

with the result reported by Tong et al.¹⁶ However, when the pH value was 3.0, the three chiral compounds have suitable retention capacity and can achieve baseline separation. So, PBS with pH 3.0 was used for the enantioselectivity of MA, MMA, and PMA.

3.1.3 | Influence of proportion of acetonitrile

The different hydro-organic mobile phases made up with water and acetonitrile were tested, and the results were summarized in Table S3. The results indicated that the values of k and α of these enantiomers gradually increased with a decrease of acetonitrile content in mobile phase containing HP- β -CD, indicating that the proportion of acetonitrile in the mobile phase obviously affected the partition coefficient of each enantiomer between stationary phase (C₁₈ column) and mobile phase^{28,29} and thus affected the k value of each enantiomer. Combined with the influence of HP- β -CD on the chromatographic retention, it can be inferred that the retention behavior of each enantiomer is driven by its partition coefficient between the mobile and stationary phases and its complexation with cyclodextrins.³⁰ This also means that the enantioselectivity is dominated by the distribution of chiral compounds between the mobile and stationary phases and the inclusion interaction between chiral compound and cyclodextrins in the chromatographic system with chiral mobile-phase additives. From Table S3, it can be also found that the column efficiency (theoretical plate number) increases with the increase of acetonitrile content in mobile phase. Although the enhancement in the column efficiency is beneficial to the improvement of the resolution factor (R_s), the decline in the α value is not conducive to improving the enantioselectivity. Finally, the R_s values of these enantiomers gradually decrease with the increase of acetonitrile content in mobile phase.

Additionally, it can be found that when the proportion of acetonitrile in the mobile phase was more than 9% (v/v), the resolution (R_s) of MA, and MMA isomers was less than 1.5, could not achieve baseline separation. In terms of economy, environmental protection, separation effect, and retention time, the optimal mobile phase is the ratio of acetonitrile and phosphate buffer (0.1 mol l⁻¹, pH 3.0) containing 15-mmol l⁻¹ HP- β -CD is 5:95 (v/v).

3.1.4 | Influence of column temperature

In the above optimal mobile phase, the influence of column temperature on enantioseparation of MA,

MMA, and PMA was further investigated, and the findings were listed in Table S4. The findings revealed that the k and α values declined gradually with rising column temperature, which is responsible for the decline in the partition coefficient of solutes between stationary phase and mobile phase. However, with rising temperature, the R_s values of MA and MMA declined whereas the R_s value of PMA increased. To our knowledge, the resolution factor is proportional to the square root of theoretical plate number (N), $(\alpha - 1)/\alpha$, and proportional to $k/(1 + k)$. Obviously, the decline in the α values with rising temperature is not good for improving the resolution factor. Nevertheless, the rising temperature can increase the diffusion coefficient of solute in the mobile phase and stationary phase and thus accelerates the partitioning between the two phases, resulting in the increase in the theoretical plate number and in favor of the enhancement in the resolution factor (R_s).³¹ This indicates that the influence of column temperature on the resolution factor (R_s) of these chiral compounds is quite complicated, resulting in the increase in the R_s value for PMA with higher k value and the decrease in the R_s value for MA and MMA with smaller k value. This also means that the kinetic factors (theoretical plate number) play a leading role in the effect of column temperature on the R_s value for PMA whereas the thermodynamic factors (such as k and α values) play a leading role in the effect of column temperature on the R_s value for MA and MMA.

Meanwhile, considering the resolution factor and analytic time as well as column life, the selected column temperature of 30°C is suitable for simultaneous analysis of MA, MMA, and PMA.

3.1.5 | Influence of flow rate

The effect of flow rate on the enantioselectivity of the selected MA and its derivatives was investigated using PBS (0.1 mol l⁻¹, pH 3.00) containing 15-mmol l⁻¹ HP- β -CD with 5% acetonitrile as the mobile phase. As shown in Table S5, with the increase of flow rate, the values of k , α , R_s , and N of these enantiomers gradually decreased. It is well known that the theoretical plate number is used to quantitatively represent the separation efficiency of chromatographic columns. Considering the impact of the above factors, this article chose 0.6 ml min⁻¹.

Through the above experiments, the results showed that the optical isomer of MA, MMA, and PMA can be separated well under the selected chromatographic conditions as shown in Figure 3.

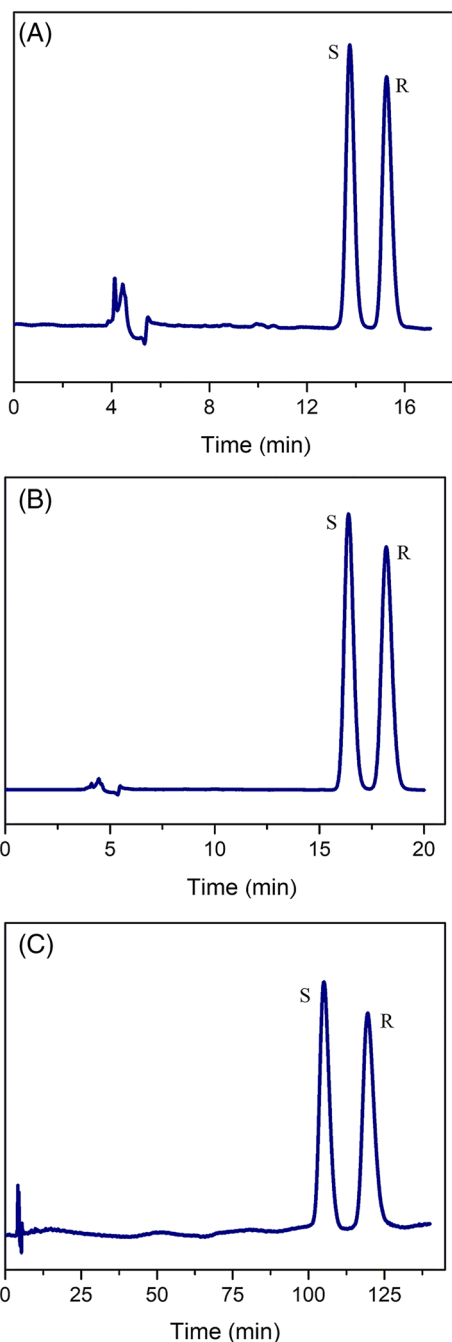


FIGURE 3 Chromatograms of enantioseparations of (A) mandelic acid, (B) 4-methoxymandelic acid, and (C) 4-propoxymandelic acid enantiomers. Chromatographic conditions: mobile phase: acetonitrile:PBS (0.1 mol l⁻¹, pH 3.00) containing HP- β -CD (15 mmol l⁻¹) = 5:95 (v/v). Flow rate: 0.6 ml min⁻¹; detection wavelength: 230 nm; column temperature: 30°C

3.2 | Assessment on thermodynamic parameters

The relationship between the retention factor (k) or separation factor (α) and the column temperature (T) during chromatographic chiral separation process can be

described by the Gibbs–Helmholtz and van't Hoff equations as follows^{28,29}:

$$\ln k = -\frac{\Delta H}{RT} + \frac{\Delta S}{R} + \ln \phi, \quad (1)$$

$$\ln \alpha = -\frac{\Delta(\Delta H)}{RT} + \frac{\Delta(\Delta S)}{R}, \quad (2)$$

$$\Delta G = \Delta H - T\Delta S, \quad (3)$$

where k is the capacity factor of enantiomers and α is the separation factor between (R)-isomer and (S)-isomer. ΔG , ΔH , and ΔS represent the Gibbs free energy change, the enthalpy change, and the entropy change, respectively. ϕ is the phase ratio. The experimental results showed that there was a good linear correlation between $\ln k'$ and $1/T$ for these isomers (Figure 4), suggesting that the ΔH and ΔS values were invariable over the entire temperature range studied and the chiral recognition mechanism for MA, MMA, and PMA under selected chromatographic system was unchanged. To our knowledge, in the traditional reversed-phase chromatography system, (R/S)-isomers have the same k values; thus, the $\Delta(\Delta H)$ and $\Delta(\Delta S)$ values between (R/S)-isomers are zero. Nevertheless, as shown in Table 1, in the reversed-phase chromatographic system with HP- β -CD chiral additive, the $\Delta(\Delta H)$ and $\Delta(\Delta S)$ values between (R/S)-isomers were not zero, suggesting that the interaction of HP- β -CD with (R)-isomers and (S)-isomers is different. Due to $|\Delta(\Delta H)| > |T\Delta(\Delta S)|$, it can be deduced that the enantioseparations of MA, MMA, and PMA are enthalpy-driven processes. And we can also conclude that the chiral recognition ability of HP- β -CD was in order of

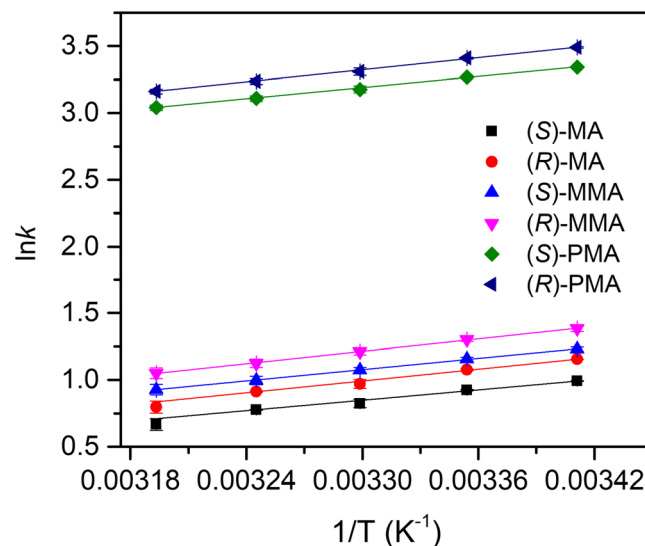


FIGURE 4 van't Hoff plots of MA, MMA, and PMA

TABLE 1 Regression parameters for Equation (1) and thermodynamic parameters

Compounds	Regression parameters for Equation (1)			ΔH (kJ mol ⁻¹)	$\Delta S + R\ln\phi$ (J mol ⁻¹ K ⁻¹)	$\Delta(\Delta H)^b$ (kJ mol ⁻¹)	$\Delta(\Delta S)^c$ (J mol ⁻¹ K ⁻¹)	$\Delta(\Delta G)^d$ (J mol ⁻¹)	
	A	B	r ^{2a}						
(R/S)-MA	k _R	1466.6	-3.8475	0.9986	-12.19	-31.99	-1.42	-3.52	-353.44
	k _S	1294.9	-3.4249	0.9987	-10.77	-28.47			
(R/S)-MMA	k _R	1547.9	-3.8937	0.9977	-12.87	-32.37	-1.23	-2.92	-345.24
	k _S	1400.0	-3.5425	0.9980	-11.64	-29.45			
(R/S)-PMA	k _R	1511.2	-1.6630	0.9974	-12.56	-13.83	-0.99	-2.16	-335.52
	k _S	1392.1	-1.4037	0.9977	-11.57	-11.67			

^aRegression parameters for Equation (1), where A is equal to $\Delta H/R$, B is equal to $\Delta S/R + \ln\phi$, r is correlation coefficient, and R is gas constant (8.314 J mol⁻¹).

^b $\Delta(\Delta H)$ is calculated by ΔH_R and ΔH_S .

^c $\Delta(\Delta S)$ is calculated by $\Delta S_R + R\ln\phi$ and $\Delta S_S + R\ln\phi$.

^d $\Delta(\Delta G)$ is calculated by $\Delta G = \Delta H - T\Delta S$ at 303 K.

MA > MMA > PMA. Additionally, the mode of interaction between small molecule and macromolecule can be deduced on the basis of the signs of the thermodynamic parameters like ΔH and ΔS . Generally, the negative values of both ΔH and ΔS represent that the main force is van der Waals force and/or hydrogen-bonding interaction. The positive values of both ΔH and ΔS mean that the main interaction force is a hydrophobic interaction. ΔH of almost zero and the positive value of ΔS represent that the main interaction force is an electrostatic force.³² Therefore, we deduced that the main mode of the interaction of HP- β -CD with MA, MMA, and PMA was van der Waals and hydrogen-bonding interactions.

3.3 | Molecular simulation

As mentioned in the assay of thermodynamic parameters, the interaction between enantiomers and chiral selector, HP- β -CD plays a significant role in the process of chiral separation. The research on the chiral resolution mechanism of enantiomers on CD and its derivatives has aroused great attention.³²⁻³⁶ To clarify the chiral resolution mechanism of (R/S)-MA, (R/S)-MMA, and (R/S)-PMA on HP- β -CD, the inclusion of HP- β -CD with each optical isomer was explored with help of molecular docking and MD approaches. First, the inclusion between HP- β -CD and each optical isomer was imitated using semiflexible docking, and thus, each enantiomer-HP- β -CD complex with the lowest binding energy was obtained. To obtain the more accurate geometry of each inclusion complex, each enantiomer-HP- β -CD complex obtained from molecular docking was used as initial structure for MD simulation.

In MD simulation, the root-mean-square deviation (RMSD) for each enantiomer-HP- β -CD in complex was calculated, and the results of MD simulation were shown

in Figure S1. As shown in Figure S1, the fluctuation range of the RMSD value of each enantiomer is about 0.1 nm, which signifies the minimal deviation with stabilized conformational coordinates.³⁷ Subsequently, the representative conformation with the lowest energy for each complex was extracted by cluster analysis (cutoff 0.3 nm) during the 120-nsec dynamic simulations and was represented in Figure 5. The findings revealed that each enantiomer embedded into the hydrophobic cavity of HP- β -CD. The phenyl, methoxyphenyl, and propoxyphenyl groups were situated in the narrow edge of HP- β -CD, whereas the -COOH moiety is situated in the wider edge. And the insertion depth of (S)-isomer was larger than that of (R)-isomer, suggesting that the inclusion of (S)-isomer with HP- β -CD was stronger than that of (R)-isomer.

Additionally, the shape of HP- β -CD has been significantly deformed as shown in Figure 5 and Table S6. And the shape of the cavities in each inclusion complex is also different. The conformational change can favor the inclusion interaction between HP- β -CD and isomers to ensure a better inclusion and enhance the complexation entropy. This conformational change is defined as "induced-fit mechanism."³⁸ In addition, the change was closely related to the structure of guest molecules; that is, the alteration in the conformation of HP- β -CD was different for the different guest molecules. Thus, it can be inferred that the flexibility of HP- β -CD played a dominative role in the chiral recognition.

3.4 | Interaction forces between HP- β -CD and isomers

As everyone knows, the inclusion interaction between guest molecule and CDs includes various noncovalent

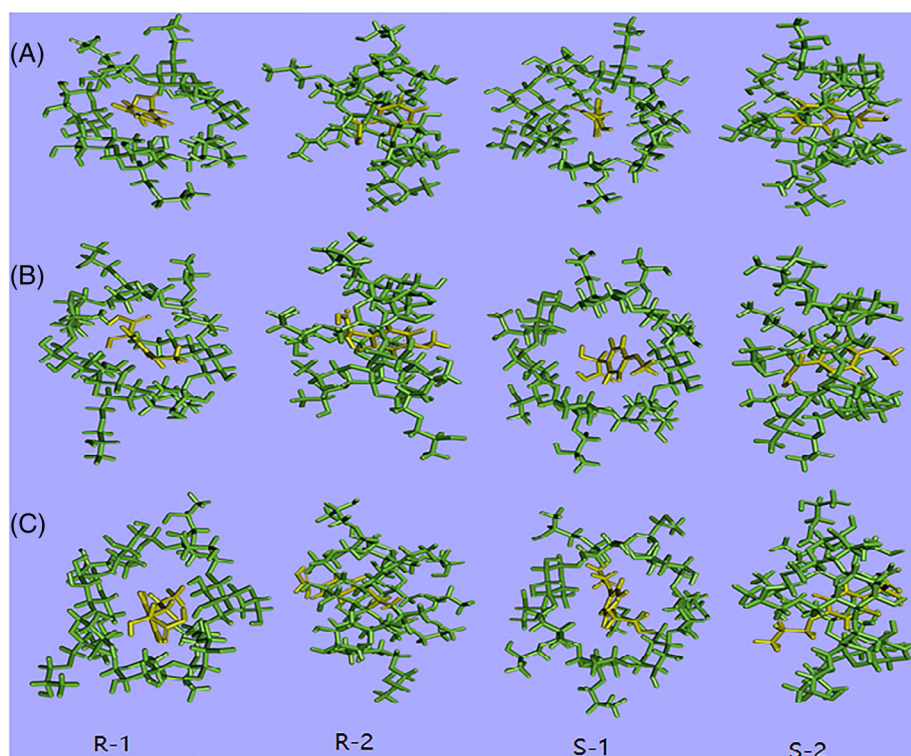


FIGURE 5 Representative geometries of complexes of HP- β -CD with (A) mandelic acid, (B) 4-methoxymandelic acid, and (C) 4-propoxymandelic acid obtained by MD simulation. (R)-1 and (S)-1 were abstracted from the wider edge of the HP- β -CD cavity, and (R)-2 and (S)-2 were abstracted from the side of the HP- β -CD wall. R and S represented (R)-isomer and (S)-isomer, respectively

TABLE 2 Various energies of various complexes obtained by molecular dynamics using MM-PBSA method^a

Complexes	ΔE_{vdw}	ΔE_{elec}	ΔE_{polar}	ΔE_{sasa}	$\Delta E_{binding}$	$\Delta(\Delta E_{binding})$
(R)-MA-HP- β -CD	-61.140 ± 1.133	-15.017 ± 0.439	42.442 ± 0.698	-6.697 ± 0.107	-40.312 ± 1.043	22.111 ± 0.73
(S)-MA-HP- β -CD	-92.176 ± 0.372	-15.637 ± 0.316	54.537 ± 0.349	-9.162 ± 0.022	-62.423 ± 0.304	
(R)-4-MMA-HP- β -CD	-120.203 ± 0.350	-10.616 ± 0.301	53.920 ± 0.430	-10.517 ± 0.027	-69.389 ± 0.345	4.425 ± 0.009
(S)-4-MMA-HP- β -CD	-112.003 ± 0.326	-18.942 ± 0.371	67.972 ± 0.428	-10.856 ± 0.024	-73.814 ± 0.354	
(R)-4-PMA-HP- β -CD	-113.647 ± 1.141	-20.188 ± 0.634	64.413 ± 0.634	-11.762 ± 0.028	-81.169 ± 0.391	1.982 ± 0.047
(S)-4-PMA-HP- β -CD	-114.816 ± 0.358	-16.631 ± 0.303	60.240 ± 0.341	-11.930 ± 0.026	-83.151 ± 0.344	

^a ΔE_{vdw} denotes van der Waals energy; ΔE_{elec} is electrostatic energy including all electron delocalizations; ΔE_{polar} is polar solvation energy; ΔE_{sasa} is SASA energy, where SASA is defined as a surface area of macromolecules that is accessible to aqueous solvent; $\Delta E_{binding}$ is binding energy; and $\Delta(\Delta E_{binding})$ is calculated by $\Delta E_{binding,R} - \Delta E_{binding,S}$. All physical quantities are kJ mol^{-1} in units.

bond interactions. The interaction energies were analyzed for each inclusion complex of 20- to 100-nsec trajectory of MD simulation using MM-PBSA approach in GROMACS and APBS1 software. Generally speaking, the MM-PBSA method cannot be completely consistent with the experimental results, but it can qualitatively analyze the main sources of contribution in chiral recognition.³⁹ As is well known, in the process of the interactions between host and guest, the main interaction forces have van der Waals force, electron delocalization interaction, solvent-accessible surface area (SASA) interaction, and the polar solvation interaction. Electron

delocalization interactions include hydrogen-bonding and dipole-dipole interaction. SASA energy represents the transfer free energy required to transfer macromolecule from aqueous solvents to nonpolar solvents.³⁷

From Table 2, it can be found that the interaction forces included the contribution of various forces is different in each isomer and HP- β -CD interaction, the van der Waals force, electron delocalization energy, and SASA energy favored of the formation of inclusion complex whereas the polar solvation energy was not favor to inclusion interaction. This was consistent with the result obtained by the analysis of thermodynamic parameters.

The binding energy of HP- β -CD with (*S*)-isomer for three chiral compounds is more negative than that with (*R*)-isomer, suggesting that the interaction between HP- β -CD and (*S*)-isomer was stronger than that of (*R*)-isomer, resulting that the concentration of (*S*)-isomer in mobile phase was larger than that of (*R*)-isomer, and thus, (*S*)-isomer is first washed out. This is consistent with the experimental results. Meanwhile, it can be also seen that the $\Delta(\Delta E_{\text{binding}})$, $(\Delta(\Delta E_{\text{binding}}) = \Delta E_{\text{binding},R} - \Delta E_{\text{binding},S})$ value was in order of MA-HP- β -CD complex > MMA-HP- β -CD complex > PMA-HP- β -CD complex, indicating that the chiral recognition ability of HP- β -CD was in order of MA > MMA > PMA. It was consistent with the order of $\Delta(\Delta G)$ values obtained from van't Hoff plot (Table 1), suggesting that the MD may be used to predict the chiral recognition ability of HP- β -CD and provide a certain degree of reference for the identification of chiral drugs in the future.

4 | CONCLUSION

The enantioseparations and chiral recognition mechanism of MA, MMA, and PMA were investigated by reversed-phase HPLC using HP- β -CD as chiral selector and by MD simulation approach. The results revealed that there was a good separation efficiency between (*R/S*)-isomers of the three compounds ($R_s > 1.5$) under selected chromatographic conditions, indicating that HP- β -CD possessed good chiral recognition ability for the three chiral compounds. The chiral recognition was responsible for forming inclusion complexes of (*R/S*)-isomers with HP- β -CD with the different conformation and binding energy. The binding energy of HP- β -CD with (*S*)-isomer for three chiral compounds is more negative than that with (*R*)-isomer, suggesting that the elution order was (*S*)-isomer > (*R*)-isomer. It is proved that the study on elution order of enantiomers through molecular simulation approach is technically feasible. In the process of the formation of inclusion complex, the main interaction energies included ΔE_{vdw} , ΔE_{elec} , ΔE_{sasa} , and ΔE_{polar} . Meantime, it can be revealed from the theoretical calculation results that the chiral recognition ability of HP- β -CD was in order of MA > PMA > MMA. It was consistent with the order of $\Delta(\Delta G)$ values obtained from van't Hoff plot (Table S6), suggesting that the MD may be used to predict the chiral recognition ability of HP- β -CD.

ACKNOWLEDGMENT

This study was funded by Huahai Pharmaceutical Co., Ltd. (YX-KF-[2005]018).

ORCID

Jie-Hua Shi  <https://orcid.org/0000-0002-9807-5654>

REFERENCES

1. Maier NM, Franco P, Lindner W. Separation of enantiomers: needs, challenges, perspectives. *J Chromatogr A*. 2001;906(1-2): 3-33.
2. Zhang J, Mao H, Li M, Su E. Cyclodextrin glucosyltransferase immobilization on polydopamine-coated Fe₃O₄ nanoparticles in the presence of polyethyleneimine for efficient β -cyclodextrin production. *Biochem Eng J*. 2019;150:107264.
3. Saenger WR, Jacob J, Gessler K, et al. Structures of the common cyclodextrins and their larger analogues—beyond the doughnut. *Chem Rev*. 1998;98(5):1787-1802.
4. Santana ACSGV, Nadvorny D, Passos TDD, Soares MFDLR, Soares-Sobrinho JL. Influence of cyclodextrin on posaconazole stability, release and activity: improve the utility of the drug. *J Drug Deliv Sci Tec*. 2019;53:101153.
5. Shi X, Zhou Y, Liu F, Mao J, Zhang Y, Shan T. Modeling of chiral gas chromatographic separation of alkyl and cycloalkyl 2-bromopropionates using cyclodextrin derivatives as stationary phases. *J Chromatogr A*. 2019;1596:161-174.
6. Ye J, Yu W, Chen G, Shen Z, Zeng S. Enantiomeric separation of 2-arylpropionic acid nonsteroidal anti-inflammatory drugs by HPLC with hydroxypropyl- β -cyclodextrin as chiral mobile phase additive. *Biomed Chromatogr*. 2010;24(8):799-807.
7. Huang Z, Guo D, Fan J, et al. HPLC semi-preparative separation of diclazuril enantiomers and racemization in solution. *J Sep Sci*. 2020;43(7):1240-1247.
8. Casado N, Saz JM, García MÁ, Marina ML. Modeling-based optimization of the simultaneous enantiomeric separation of multicomponent mixtures of phenoxy acid herbicides using dual cyclodextrin systems by capillary electrophoresis. *J Chromatogr A*. 2019;1610:460552.
9. Deng M, Li S, Cai L, Guo X. Preparation of a hydroxypropyl- β -cyclodextrin functionalized monolithic column by one-pot sequential reaction and its application for capillary electrochromatographic enantiomer separation. *J Chromatogr A*. 1603;2019:269-277.
10. Tang K, Zhang P. Enantioselective extraction of terbutaline enantiomers with β -cyclodextrin derivatives as hydrophilic selectors. *Chem Pap*. 2011;65:273-279.
11. Hadjmohammadi MR, Hashemi M. Chiral separation of methadone using solid membrane extraction based on chiral selector, solid membrane: sheep skin leather. *J Iran Chem Soc*. 2019; 16(8):1611-1616.
12. Tang C-D, Shi H-L, Jia Y-Y, et al. High level and enantioselective production of L-phenylglycine from racemic mandelic acid by engineered *Escherichia coli* using response surface methodology. *Enzyme Microb Technol*. 2020;136: 109513.
13. Blay G, Fernández I, Monje B, Muñoz MC, Pedro JR, Vila C. Enantioselective synthesis of 2-substituted-1,4-diketones from (*S*)-mandelic acid enolate and α,β -enones. *Tetrahedron*. 2006; 62(39):9174-9182.
14. Zang J, Wang ZJ, Wu YZ. The optical resolution of mandelic acid. *Fine Chem Intermedia Tes*. 2005;35:50-52.

15. Hallas G, Yoon C. The synthesis and properties of naphthodifuranones and naphthofuranonepyrrolidones. *Dyes Pigments*. 2001;48(2):121-132.
16. Tong S, Zhang H, Shen M, Ito Y, Yan J. Enantioseparation of mandelic acid derivatives by high performance liquid chromatography with substituted β -cyclodextrin as chiral mobile phase additive and evaluation of inclusion complex formation. *J Chromatogr B*. 2014;962:44-51.
17. Tong SQ, Shen MM, Xiong Q, Wang XP, Lu MX, Yan JZ. Chiral ligand exchange countercurrent chromatography: equilibrium model study on enantioseparation of mandelic acid. *J Chromatogr A*. 2016;1447:115-121.
18. Shi JH, Su YH, Jiang W. Enantioseparation and chiral recognition of α -cyclohexylmandelic acid and methyl α -cyclohexylmandelate on hydroxypropyl- β -cyclodextrin as chiral selector: HPLC and molecular modelling. *J Chromatogr Sci*. 2013;51(1):8-16.
19. Shi JH, Ding ZJ, Hu Y. Experimental and theoretical studies on the enantioseparation and chiral recognition of mandelate and cyclohexylmandelate on permethylated β -cyclodextrin chiral stationary phase. *Chromatographia*. 2011;74(3-4):319-325.
20. Zhang P, Feng X, Tang K, Xu W. Study on enantioseparation of α -cyclopentyl-mandelic acid enantiomers using continuous liquid-liquid extraction in centrifugal contactor separators: experiments and modelling. *Chem Eng Process*. 2016;107:168-176.
21. Kellici TF, Ntountaniotis D, Leonis G, et al. Investigation of the interactions of silibinin with 2-hydroxypropyl- β -cyclodextrin through biophysical techniques and computational methods. *Mol Pharm*. 2015;12(3):954-965.
22. Zhao Q, Gao H, Su Y, et al. Experimental characterization and molecular dynamic simulation of ketoprofen-cyclodextrin complexes. *Chem Phys Lett*. 2019;736:136802.
23. Tripathi MK, Yasir M, Gurjar VS, Bose P, Shrivastava ADR. Insights from the molecular docking of hydrolytic products of methyl isocyanate (MIC) to inhibition of human immune proteins. *Interdiscip Sci*. 2015;7:287-294.
24. Wang JM, Wolf RM, Caldwell JW, Kollman PA, Case DA. Development and testing of a general amber force field. *J Comput Chem*. 2004;25(9):1157-1174.
25. Andersen HC. Molecular dynamics simulations at constant pressure and/or temperature. *J Chem Phys*. 1980;72(4):2384-2390.
26. Wang R, Zhou H, Siu SWI, Gan Y, Wang Y, Ouyang D. Comparison of three molecular simulation approaches for cyclodextrin-ibuprofen complexation. *J Nanomater*. 2015;2015:193049.
27. Tang K, Chen Y, Huang K, Liu J. Enantioselective resolution of chiral aromatic acids by biphasic recognition chiral extraction. *Tetrahedron*. 2007;18(20):2399-2408.
28. Mcgachy NT, Grinberg N, Variankaval N. Thermodynamic study of *N*-trifluoroacetyl-*O*-alkyl nipecotic acid ester enantiomers on diluted permethylated β -cyclodextrin stationary phase. *J Chromatogr A*. 2005;1064(2):193-204.
29. Shi JH, Xu SX, Jia QQ, Yan XQ. Characterization of a cellulose trisphenylcarbamate/1-octyl-3-methylimidazolium tetrafluoroborate mixture as GC stationary phase: thermodynamic parameters and LSER methodology. *Chromatographia*. 2013;76(15-16):1021-1029.
30. Grillo R, de Melo NF, Moraes CM, et al. Study of the interaction between hydroxymethylnitrofurazone and 2-hydroxypropyl- β -cyclodextrin. *J Pharm Biomed Anal*. 2008;47(2):295-302.
31. Rong R, Deng Y. *Instrumental Analysis*, Second Ed. Beijing: China Medical Science Press; 2018. 180p.
32. de Miranda TM, de Oliveira AR, Pereira JR, et al. Inclusion vs. micellization in the cetylpyridine chloride/ β -cyclodextrin system: a structural and thermodynamic approach. *J Mo Struct*. 2019;1184:289-297.
33. Lipkowitz KB. Applications of computational chemistry to the study of cyclodextrins. *Chem Rev*. 1998;98(5):1829-1874.
34. Shi JH, Hu Y, Ding ZJ. Theoretical study on chiral recognition mechanism of ethyl-3-hydroxybutyrate with permethylated β -cyclodextrin. *Comput Theor Chem*. 2011;973(1-3):62-68.
35. Ali SM, Muzaffar S, Imtiaz S. Comparative study of complexation between cyclodextrins and xylazine using ^1H NMR and molecular modelling methods. *J Mol Struct*. 2019;1197:56-64.
36. Shi JH, Ding ZJ, Hu Y. Theoretical study on chiral recognition mechanism of methyl mandelate enantiomers on permethylated β -cyclodextrin. *J Mol Model*. 2012;18(2):803-813.
37. Kumari R, Kumar R, Open Source Drug Discovery Consortium, Lynn A. *g_mmpbsa*—a GROMACS tool for high-throughput MM-PBSA calculations. *J Chem Inf Model*. 2014;54(7):1951-1962.
38. Saenger W, Noltemeyer M, Manor PC, Hingerty B, Klar B. "Induced-fit"-type complex formation of the model enzyme α -cyclodextrin. *Bioorg Chem*. 1976;5(2):187-195.
39. Meng X-Y, Zhang H-X, Mezei M, Meng C. Molecular docking: a powerful approach for structure-based drug discovery. *Curr Comput Aided Drug des*. 2011;7(2):146-157.

SUPPORTING INFORMATION

Additional supporting information may be found in the online version of the article at the publisher's website.

How to cite this article: Shi J-H, Lin Z-Y, Kou S-B, Wang B-L, Jiang S-L. Enantioseparation of mandelic acid and substituted derivatives by high-performance liquid chromatography with hydroxypropyl- β -cyclodextrin as chiral mobile additive and evaluation of inclusion complexes by molecular dynamics. *Chirality*. 2021;1-10. doi: 10.1002/chir.23348